Robotic catheter cardiac ablation combining ultrasound guidance and force control

Samuel B. Kesner and Robert D. Howe

Abstract

Cardiac catheters allow physicians to access the inside of the heart and perform therapeutic interventions without stopping the heart or opening the chest. However, conventional manual and actuated cardiac catheters are currently unable to precisely track and manipulate the intracardiac tissue structures because of the fast tissue motion and potential for applying damaging forces. This paper addresses these challenges by proposing and implementing a robotic catheter system that uses 3D ultrasound image guidance and force control to enable constant contact with a moving target surface in order to perform interventional procedures, such as intracardiac tissue ablation. The robotic catheter system, consisting of a catheter module, ablation and force sensing end effector, drive system, and image-guidance and control system, was commanded to apply a constant force against a moving target using a position-modulated force control method. The control system uses a combination of position tracking, force feedback, and friction and backlash compensation to achieve accurate and safe catheter–tissue interactions. The catheter was able to maintain a 1 N force on a moving motion simulator target under ultrasound guidance with 0.08 N RMS error. In a simulated ablation experiment, the robotic catheter was also able to apply a consistent force on the target while maintaining ablation electrode contact with 97% less RMS contact resistance variation than a passive mechanical equivalent. In addition, the use of force control improved catheter motion tracking by approximately 20%. These results demonstrate that 3D ultrasound guidance and force tracking allow the robotic system to maintain improved contact with a moving tissue structure, thus allowing for more accurate and repeatable cardiac procedures.

1. Introduction

Advances in cardiac catheter technology allow physicians to treat a range of conditions inside the beating heart while avoiding both the invasiveness of opening the chest and the cognitive impairment risks associated with cardiopulmonary bypass (Roach et al., 1996; Murkin et al., 1999; Baim, 2005: 992). However, the majority of catheters currently used for cardiac interventions only allow for slow manual motions of the catheter tip and are unable to control the forces applied to the tissue surfaces. Commercially available robotic catheter systems, such as the Artisan Control Catheter (Hansen Medical, Mountain View, CA) or the CorPath Vascular Robotic System (Corindus Vascular Robotics, Natick, MA), achieve manual catheter manipulation speeds while allowing the operator to utilize robotic teleoperation to reduce radiation exposure (Camarillo et al., 2008; Jayender et al., 2008; Beyar, 2010). However, neither the manual nor the commercial robotic catheter systems are able to compensate for the fast cardiac motion or regulate the forces applied to the tissue surface.

The goal of our work is to enable a robotic catheter to track the fast motions of the heart while controlling the forces applied by the catheter end effector to the tissue in order to improve the safety and efficacy of medical procedures. This objective is achieved through the use of 3D ultrasound (3DUS) guidance, active motion compensation, and catheter tip force control. One medical application that may benefit from this technology is the radiofrequency (RF) ablation of cardiac tissue. Ablation is used by interventional cardiologists and cardiac surgeons to destroy cardiac conduction pathways that contribute to arrhythmias, or heart beat abnormalities (Huang et al., 2000). The outcome success of this procedure is dependent on the electrode contact with the tissue and force application, and therefore

Wyss Institute for Biologically Inspired Engineering at Harvard University, Boston, MA, USA

Corresponding author:
Samuel B. Kesner, Harvard School of Engineering and Applied Sciences, Cambridge, MA, USA.
Email: skesner@seas.harvard.edu

can benefit from the robotic system proposed here (Kalman et al., 1997; Okumura et al., 2007; Shah et al. 2010, 2011). In addition to cardiac ablation, other applications of this robotic system include beating heart cardiac valve repair and replacement and the delivery of implants to moving structures inside of the beating heart, such as septal defect repair implants.

In previous work, we have demonstrated *in vivo* the ability of the robotic catheter system to compensate for the fast motion of the heart (Kesner and Howe, 2011d). In addition, a custom catheter tip force sensor was developed to enable the catheter to maintain a constant force against a target (Kesner and Howe, 2012). However, the catheter force control system has to date only been evaluated on the benchtop using noise-free simulated position signals rather than noisy ultrasound image-derived signals (Kesner and Howe, 2011a, 2011c). Other work in cardiac motion compensation has focused primarily on interacting with the exterior of the beating heart (Nakamura et al., 2001; Ginhoux et al., 2005; Bebek and Cavusoglu, 2007; Richa et al., 2010). In addition, the previous work in robotic catheters has primarily focused on teleoperation and position control (Camarillo et al., 2008; Jayender et al., 2008; Beyar, 2010). To the authors' knowledge, the work presented here represents the first time 3DUS image guidance and force control has been used to enable a robotic catheter to accurately interact with a moving target. As shown below, the combination of force feedback and 3DUS servoing improves both the force and position control performance. Furthermore, this paper presents the first steps towards applying the 3DUS-guided and motion compensated catheter system to a clinical procedure, improving cardiac ablation using force control.

The following section presents the robotic catheter system, the force sensing and ablation end effector, and the force control method. Next, the paper presents the evaluation of the system, including benchtop experiments examining the control method, water tank evaluations of the image guidance force controller, and experiments evaluating the efficacy of the robotic catheter system during a simulated cardiac ablation as compared against a passive manual catheter. Finally, this paper concludes with a discussion of the implications and limitations of the results and future applications of the technology. This work demonstrates the potential benefits of integrating motion-compensation and force control with cardiac intervention catheters.

2. Technical approach

The goal of the robotic catheter system is to use real-time 3DUS to measure the target tissue motion and then drive the actuated catheter to synchronize with the motion and while interacting with and repairing a cardiac target tissue. The catheter system is designed to rapidly servo along one degree of freedom at speeds and displacements sufficient for tracking certain cardiac structures including the
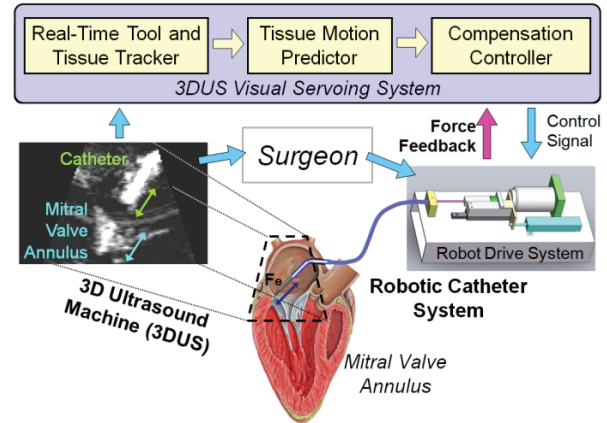

Fig. 1. The robotic system servos the catheter using 3DUS guidance and force feedback.
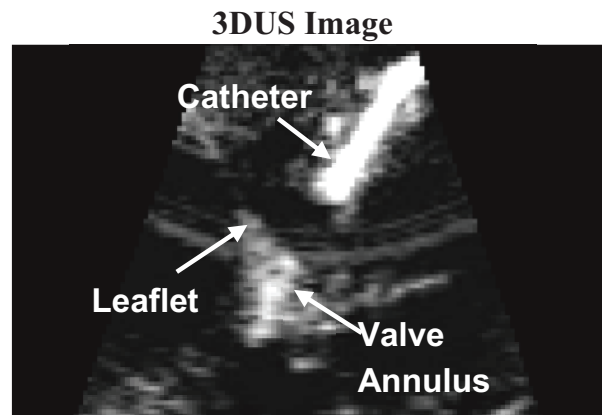

Fig. 2. Ultrasound image showing the catheter, mitral valve annulus, and mitral valve leaflets.

human mitral valve annulus (Kettler et al., 2007; Kesner and Howe, 2011d). The system (Figure 1) is composed of three main modules: the drive system that actuates the catheter, the catheter module (Figure 2) that is inserted through the vasculature into the heart, and the 3D ultrasound visual servoing system that tracks the tissue and commands the catheter to follow the motion.

The catheter drive system (Figure 1) is composed of a linear voice coil actuator (NCC20-18-02-1X, H2W Technologies Inc, Valencia, CA; 50.8 mm travel, 26.7 N peak force), a linear ball bearing slide (BX3-3, Tusk Direct, Inc., Bethel, CT), and a linear potentiometer position sensor (LP-50F, Midori America Corp, Fullerton, CA, linearity: $\pm 0.5\%$) that are able to rapidly adjust the catheter position. The catheter module consists of a sheath, a guidewire, and the end effectors required for each specific repair procedure. The sheath is an 85 cm long section of flexible Teflon or Nylon tubing that encloses the guidewire, a close-wound stainless steel spring that is easily bent but can apply significant compressive forces without buckling. During a procedure, the sheath is inserted from a peripheral blood
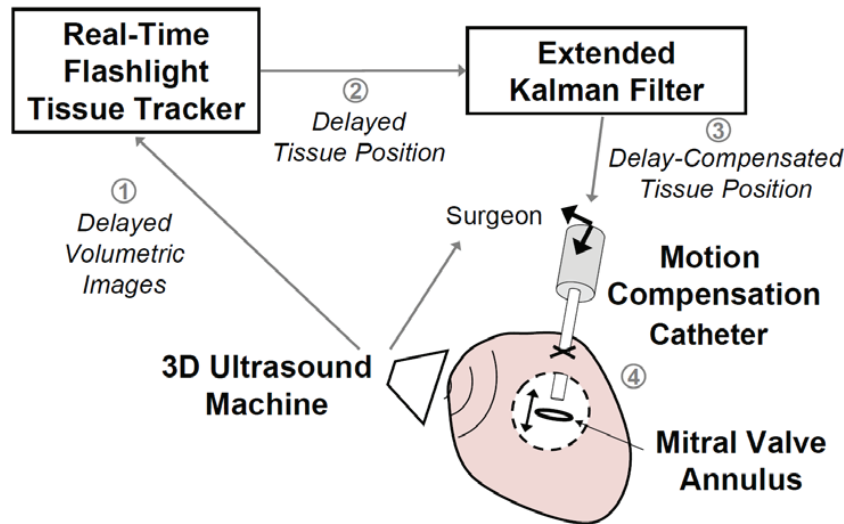
Fig. 3. The 3DUS serving system uses 3D ultrasound imaging to automatically synchronize the motion of an actuated device with a tissue target. The circled numbers indicate the order of data flow through the system: (1) The time-delayed 3DUS images, (2) the tissue positions generated by the tissue tracking algorithm, (3) the delay-compensated tissue positions, and (4) the resultant tracking position of the motion compensation catheter.
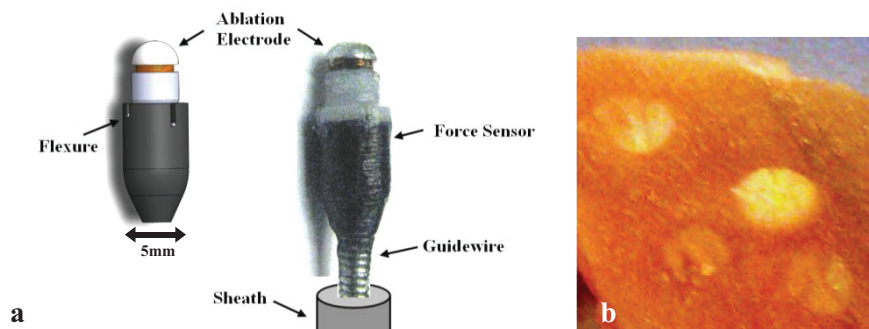

Fig. 4. (a) Ablation end effector solid model and prototype. (b) Tissue sample (porcine skeletal muscle) ablated with the RF ablation end effector. Lesions are approximately 4 mm in diameter.

vessel into the heart and then fixed in place while the drive system servos the guidewire inside the sheath to compensate for the heart motion and regulate the forces applied to the cardiac tissue.

2.1. 3D ultrasound servoing system

The visual servoing system utilizes a 3DUS machine (Figure 1, SONOS 7500 with X4 Ultrasound Transducer, Philips Healthcare, Andover, MA, USA) that streams volumes at 28 Hz and a guidance system to track and predict the tissue motion in order to determine the real-time position of the cardiac tissue and control the catheter (Novotny et al., 2007a, 2007b; Yuen et al., 2008b, 2009).

The ultrasound servoing system (Figure 3) streams 3D image volumes from the ultrasound scanner to an image processing computer via Ethernet. A GPU-based Radon transform algorithm finds the catheter axis in real-time. The target tissue is then located using the flashlight tissue tracker algorithm, which projects the instrument axis

forward through the image volume until tissue is encountered (Yuen et al., 2010). This method allows the clinician to designate the target to be tracked by simply pointing at it with the catheter. To compensate for the 50–100 ms delay in image acquisition and processing, an extended Kalman filter (EKF) estimates the current tissue location based on a Fourier decomposition of the cardiac cycle (Yuen et al., 2009). Previous *in vivo* experiments using this servoing system showed that a rigid instrument system was capable of accurate tracking within the heart, with an RMS error of 1.0 mm. A detailed description of the 3DUS visual servoing system is provided elsewhere (Novotny et al., 2007a, 2007b; Yuen et al., 2008b, 2009; Kesner et al., 2010).

2.2. Force sensor

In addition to the robotic catheter, a novel integrated force sensing and ablation end effector is presented here for the first time (Figure 4). The design goal of the ablation tool is to enable the catheter system to apply RF energy to the
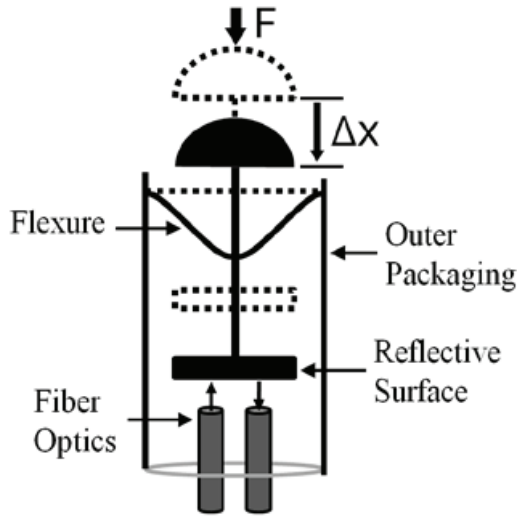
Fig. 5. Catheter tip force sensor schematic.

fast-moving tissue inside the heart while applying a constant normal force. The functional requirements of the ablation end effector are to sense forces, to ablate tissue using a clinical RF generator with a similar efficacy to conventional ablation catheters, and to be robust enough to operate in the intracardiac environment. The device consists of a force sensor described in (Kesner and Howe, 2011a), a stainless steel electrode, and a fine wire that runs through the catheter body to connect the electrode to the external RF current generator. The current prototype is approximately 5 mm in diameter and is created using rapid prototyping 3D printing technology. The size of the end effector can be further reduced with improved fabrication such as laser micromachining and metal laser sintering. Figure 4(b) presents examples of the RF ablation lesions created with this tool on porcine skeletal muscle tissue (RF generator: Stockert 70, Biosense Webster, Diamond Bar, CA). Figure 5 presents a schematic diagram of the force sensor component of the ablation end effector and example force sensor performance data. The force sensor converts applied forces into small deflections of a reflective surface supported by flexures. The reflective surface modulates the amount of light reflected back to a fiber optic sensor, which is calibrated and used to determine the amount of applied force. NiTi wires flexures (0.25 mm diameter) are arranged in a perpendicular configuration, which allows for large defections along the axis of the catheter but resists lateral deflections, has little hysteresis, and prevents rubbing of the sensor components. Superelastic NiTi flexures were selected for overload protection. A fiber optic transducer was selected for this sensor because it is inexpensive, easy to implement, and requires no electrical components within the catheter (Webster, 1988). Integrating the transducer into the sensor is as simple as inserting the fibers and fixing them in place with adhesive.

The Objet Connex500 3D printer (Objet Geometries Ltd, Billerica, MA) was used to fabricate the catheter ablation and force sensor end effector. This printer has a minimum

resolution of 16 microns and can print with a range of photopolymers, from a stiff acrylic plastic to a rubber-like, flexible plastic (see Objet Geometries Ltd, 2010). For this work, the Verowhite photopolymer was selected because it is a stiff plastic (2 GPa) with a high tensile strength (50 MPa).

The catheter tip sensor was calibrated and tested with a commercial 6-axis force torque sensor (Mini40, ATI Industrial Automation, Apex, NC). The 3D printed sensor was manually loaded against the ATI sensor with a varying force profile. The signal from the fiber optic sensor was amplified with a digital fiber amplifier (E3X-DA21-N, Omron Electronics LLC Industrial Automation, Schaumburg, IL) before digital acquisition (DAQCard-6024E, National Instruments Corp., Austin, TX). A more detail description of the 3D printed force sensor technology is provided elsewhere (Kesner and Howe, 2011a).

2.3. Force control method

The objective of the control system is to apply a desired force on a fast moving target with the robotic catheter end effector. A standard error-based force control approach will not work for the robotic catheter system because of the limitations identified in (Kesner and Howe, 2011d), including backlash and friction in the catheter transmission system (Eppinger and Seering, 1987; Townsend and Salisbury Jr, 1987). To overcome these issues, we propose a method that uses the force error term to modulate the commanded position trajectory of the catheter. This approach is similar to the inner position loop force control approaches used to implement force control on high-friction industrial manipulators (Maples and Becker, 1986) and methods presented by Villani and coworkers (Chiaverini et al., 1999). This approach results in improved system stability and allows for the controller to directly compensate for the catheter friction and backlash in the inner position loop as these limitations are position and velocity dependent (Kesner and Howe, 2011d). See Figure 6 for a block diagram of the control system.

In this force control approach, the drive system is commanded to follow a desired position, x_d, that is the sum of the position of the moving target, x_e and the position offset required to maintain the desired force, x_f

$$x_d = x_e + x_f \qquad (1)$$

The force modulation term is

$$x_f = K_f(F_d - F_e) + K_{fi} \int (F_d - F_e) \, dt \qquad (2)$$

where F_d is desired force, F_e is the force applied to the environment, and K_f and K_{fi} are controller gains. The drive system is commanded to follow the desired position trajectory with a standard PID controller running at 1 kHz.
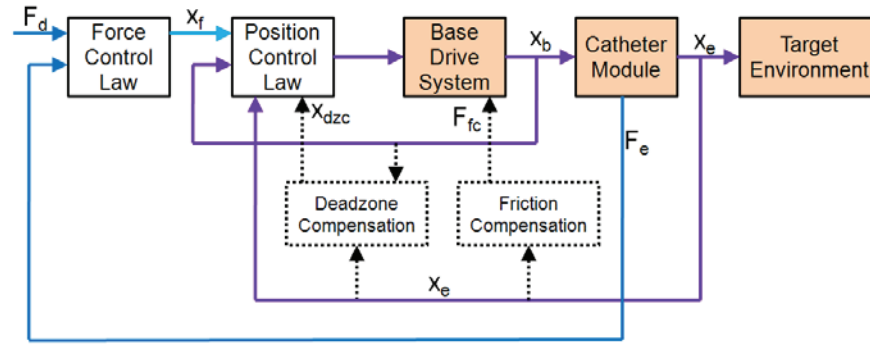
Fig. 6. The force control system block diagram. The control system uses force and position feedback as well as compensation terms to command the catheter to maintain a desired force on a moving target.

2.4. Compensation methods

Compensation terms are introduced to the position feedback loop to improve the control system performance, indicated in the block diagram in Figure 6 by dotted lines (Kesner and Howe, 2011d). Friction compensation assumes a Coulombic friction model for the catheter and then feeds forward the friction force F_{fc}, based on an observer that predicts the velocity (Kesner and Howe, 2011d). The friction force is determined during operation through an estimation routine that utilizes the motor current values and is dominated by the catheter system design (materials, geometry) and sheath configuration bend angle (θ). The bend angle (θ) can be determined during a procedure using a number of methods, including bend sensors embedded along the length of the catheter sheath (Prisco, 2012), electromagnetic tracking (Wilson et al., 2008), and the extraction of catheter bend angle information from medical images (most likely X-ray fluoroscopy) during the procedure. Backlash compensation adds an additional term to x_d that adjusts the desired base position to overcome the deadzone behavior in the catheter module. The amount of compensation, x_{dzc}, is determined using a catheter-specific deadzone model presented in (Kesner and Howe, 2011d):

$$x_{dzc} = \theta(D_{sh} - D_{gw}) \qquad (3)$$

where D_{sh} is the inner diameter of the sheath and D_{gw} is the diameter of the guidewire. The compensation term x_{dzc} is either added or subtracted from x_d based on the direction of target motion and the position of the guidewire relative to the deadzone region. While the deadzone value is sensitive to the bend angle, this parameter can be accurately measured with the methods described above and will not vary greatly over the course of a procedure as the sheath is constrained by the vasculature between the entry site and the heart.

2.5. Force controller limitations

The performance of the force control method described here is limited by a number of factors, including the accuracy of the tissue motion tracking, the compensation terms, and the unmodeled effects of the environment.

The most significant limitation of the controller is its dependence on accurate target motion information for motion compensation and force regulation. The controller relies on the periodic motion of the cardiac tissue to enable accurate predictive position estimations (Yuen et al, 2008b; Kesner and Howe, 2011d). If the tissue motion deviates greatly from the previous periodic trajectory, the desired position (x_d) component of the position control loop will be incorrect because the estimated position of the environment (x_e) will not match the real tissue motion. Possible sources of target motion tracking errors include external disturbances like arrhythmias or ectopic beats, unmodeled motions like respirations, changes in the tissue motion due to the forces applied by the catheter, and failures of the motion prediction algorithm to converge on the correct trajectory due to poor imaging quality or tool positioning (Yuen et al., 2008a, 2009; Kesner and Howe, 2011d).

Another limitation of the force controller arises from changes to the physical catheter system. The controller assumes a static model for the system performance parameters for a given catheter configuration. For example, the friction forces and backlash parameters are fixed for each catheter position and orientation. While assuming a static catheter configuration is reasonable while operating in the constrained workspace inside the heart, other factors, such as blood clots developing between the catheter guidewire and sheath, can change the friction and backlash model parameters. To overcome these model limitations, the backlash and friction are determined once the catheter is in position but before it has engaged the tissue to include any effects from recent changes in the system or configuration.

In certain situations, the model-predicted deadzone width must be increased to account for the deformation of the sheath and guidewire caused by significant catheter friction (Kesner and Howe, 2011d). This change in the backlash is generated by increased internal catheter friction that causes the guidewire to deform and buckle as it moves, thus increasing the backlash behavior of the catheter tip. In this study, x_{dzc} was doubled for certain trials to account for
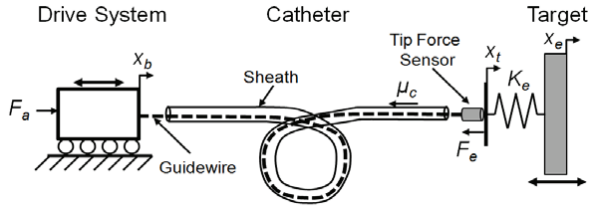
Fig. 7. Benchtop evaluation experimental setup.

the increased deadzone width caused by significant friction values as high as 2 N. The decision to double the backlash compensation term was selected empirically based on our previous investigations of the catheter friction-backlash behavior. This friction-dependent backlash behavior has been reported in previous work (Kesner and Howe, 2010, 2011d).

3. Benchtop experimental evaluation

The force control methods proposed above were first evaluated on the benchtop to characterize the system and determine how well the catheter can maintain a desired force against a fast moving target. Based on our previous studies of fast motion compensation. With a catheter, the important experimental variables to examine are the catheter bend angle (θ) and the speed and trajectory of the target (Kesner and Howe, 2011d). See Figure 7 for a diagram of the benchtop experimental setup used to evaluate the controller designs. Ground truth values were determined using a number of appropriate sensing modalities, including electromagnetic trackers (3D Guidance trakSTAR system, Ascension Technology Corporation, Milton, VT) to measure the catheter tip trajectory, a linear potentiometer position sensor integrated into the motion simulator mechanism to sense the target position, and a commercial force sensor (LCFD-1KG, Omega Engineering, Stamford, CT; range: 10 N, accuracy: +/–0.015 N) and the catheter force sensor to determine the applied force values.

The first set of experiments examined the performance of the force control schemes while interacting with a target following a 12 mm peak-to-peak, 1 Hz sinusoidal trajectory in three sheath bend configurations: $0°$, $180°$, and $360°$. The friction, modeled as simple Coulombic friction, increases approximately linearly with bend angle (Kesner and Howe, 2010). The width of the backlash deadzone, described in equation (3), is also a function of the bend angle and can be accurately predicted with the deadzone width model first presented in (Kesner and Howe, 2010).

A sinusoidal trajectory was selected as an initial experimental evaluation trajectory because it is the dominant component of cardiac motion, as demonstrated by the spectral decomposition in (Kettler et al., 2007). For a more realistic experiment, a human mitral valve annulus trajectory was also used below to evaluate the system (Kettler et al., 2007).
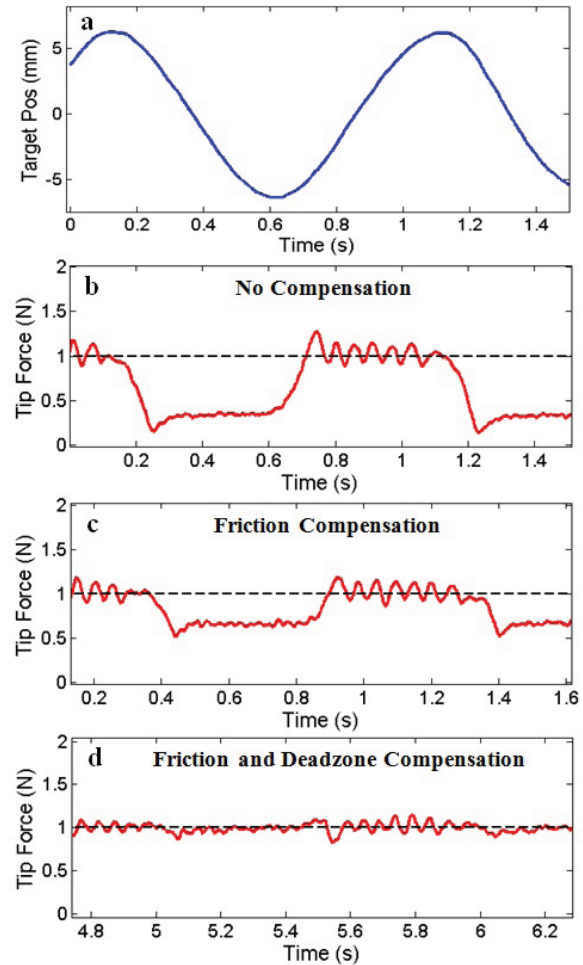

Fig. 8. Sinusoid trajectory comparison. (a) 1 Hz sinusoidal target trajectory and (b) the catheter tip force with only force-modulated position control, (c) with the addition of friction compensation, and (d) with the addition of both friction and deadzone compensation. The bend angle is $360°$.

To evaluate the performance of the proposed force control methods, the system was tested with three controller configurations: (i) the force-modulated position controller in equation (2), (ii) the controller with an added friction compensation term, and (iii) the controller with both friction and deadzone compensation terms. The force-modulation gains, K_f and K_{fi}, were tuned for best stable performance and kept constant for all of the experiments.

3.1. Force control methods comparison

Figure 8 presents a comparison of the controller performance applying a constant force (1 N) against the motion simulator target with the catheter in a $360°$ bend configuration. The target was covered with a compliant foam with a stiffness (K_e) of approximately 0.25 N/mm to simulate cardiac tissue.
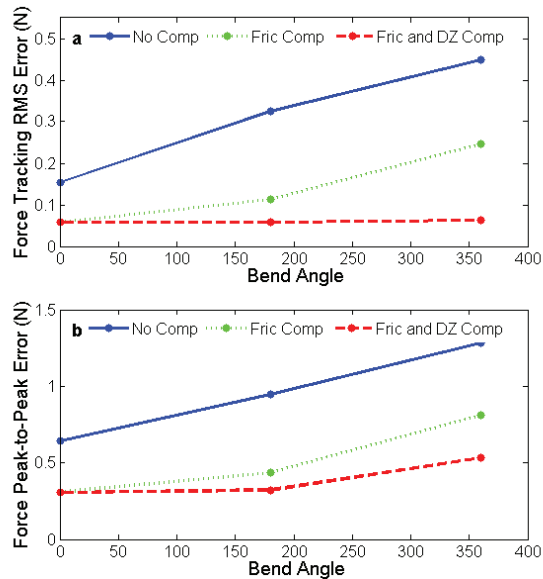
Fig. 9. (a) Force tracking RMS error and (b) force tracking peak-to-peak error against a 1 Hz sinusoidal target as a function of bend angle for the three force control methods.

Fig. 10. (a) Force tracking RMS error and (b) peak-to-peak error while tracking a sinusoidal trajectory as a function of the target frequency.

The results in Figure 8 demonstrate that both friction and deadzone compensation greatly improve the force tracking. Significant tracking errors can be seen when the target changes direction in both Figure 8(b) and (c). These errors are because the controllers in these plots do not compensate for the deadzone region behavior. Experimentally, this behavior appears as if the tip of the catheter is delayed in responding to the changes in the target trajectory. Deadzone compensation, demonstrated in Figure 8d, significantly improves the tracking by adjusting the desired position to remove the backlash effects of the deadzone. Friction compensation also improves tracking by cancelling the friction resistance in the sheath, as seen in the improvement in performance between Figure 8(b) and (c).

Figure 9 summarizes the performance results of the three force controllers for each of the three catheter configurations. The average performance of each the controllers, presented in Figure 9(a) as the RMS deviation from the desired force, shows that the compensation terms significantly improve the catheter system's force tracking ability. For example, the RMS error for the 360° bend configuration decreases by over 45% when friction compensated was added and by almost 86% when both friction and deadzone compensated were added.

The maximum deviations from the desired force are expressed as the peak-to-peak value, the difference between the maximum and minimum tip force value during each experiment. These deviations are often greatest during the changes in the target's direction of motion (Figure 8). This data, presented in Figure 9(b), clearly indicates that the compensation methods reduce the deviations from the desired force. For example, friction and backlash
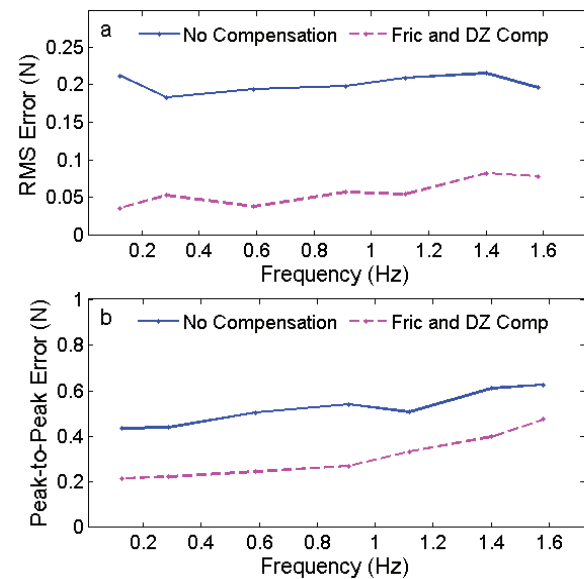
compensation decreased the peak-to-peak variations in the 360° bend configuration by almost 60%. It should be noted that for the 0° catheter bend configuration, the deadzone compensation does not alter the RMS or peak-to-peak values because the catheter system has no deadzone according to the backlash model in equation (3).

The effect of the frequency of the sinusoidal target was also investigated in this study. The target frequency was varied from 0.1–1.6 Hz, approximately the range of possible heart rates encountered during clinical procedures (6–96 BPM). The catheter was constrained in a 180° bend configuration and the control system was commanded to maintain a desired force of 1 N with and without friction and deadzone compensation.

The results of these experiments are summarized in Figure 10. The RMS error for both controllers was approximately constant across the frequency range, with the compensated controller performing roughly 75% better than the uncompensated controller for all of the frequencies. The peak-to-peak error increased as a function of the frequency. This trend is because, as the frequency increases, the speed at which the catheter must travel through the deadzone to maintain the desired force also increases.

4. 3D ultrasound-guided performance evaluation

The force controlled catheter system was also evaluated in water tank studies under 3DUS guidance. A water tank is required to evaluate the visual servoing system because clinical ultrasound machines cannot operate in air.
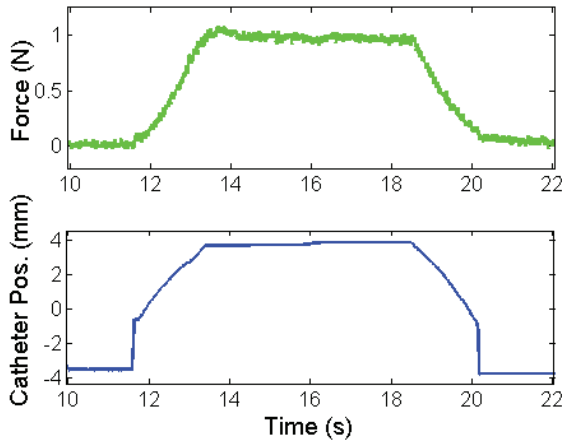
Fig. 11. Engaging the target: The catheter engages and retracts from a static target using a trapezoidal trajectory to achieve the desired force.

Fig. 12. The catheter tip immediately pulls back into a safe position if the force threshold (1.5 N) is exceeded to prevent tissue damage.

4.1. Engaging the target

One of the challenges of regulating the forces applied by the catheter tip to a target is the transition from operating in free space to applying the desired force on the fast-moving target.

The process of engaging a surface is challenging because of the potential for the catheter tip to apply large and destabilizing interaction forces. Furthermore, the catheter must be able to safely retract from the target surface after the experiment is completed. To ensure that the catheter contacts the target in a controlled manner, a trapezoidal position trajectory is commanded to dictate the processes by which the tool engages and retracts from the target.

It is assumed that the catheter must maintain a constant force against the tissue in order to apply a surgical technique such as ablate, resect, or staple the tissue. In the method used here, the catheter approaches the surface at a rate of 2.5–5 mm/s, applies the desired force for 5 s, and then retracts from the tissue at 5 mm/s. Figure 11 demonstrates engaging a static target. An alternative engagement process is for the user to manually adjust the catheter position until it makes first contact with the moving tissue and then switch to a force control method to maintain a constant interaction force.

The process of engaging a target is further complicated when the target is quickly moving, such as the mitral valve annulus (Kettler et al., 2007). If the approach process does not consider the motion of the target and progresses at a constant velocity, the catheter tip may collide with the target surface and result in a large spike of force and possibly system instability. To prevent this issue, the moving target is virtually stabilized relative to the catheter tip by utilizing motion compensation during the approach procedure.

To prevent damage to the tissue or tool caused by instability or unexpected forces applied to the catheter tip, the controller is instructed to pull back the catheter and enter a "safe mode" if a larger than expected force is sensed at
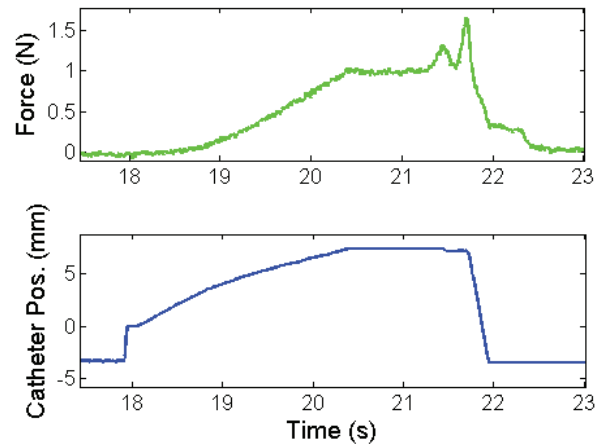
the tip. As demonstrated in Figure 12, the catheter withdraws at a speed of 50 mm/s when a force spike is recorded at the tip. This force spike, created by quickly hitting the tip of the catheter force sensor, simulates an ectopic heart beat not anticipated by the motion compensation controller, causing the catheter tip to collide with the heart wall. The force threshold, in this case 1.5 N, determines if the controller needs to pull back the catheter into the safe mode. For comparison with this damage prevention method, see Kesner and Howe (2011b) for examples of the collision forces experienced by a catheter without force compensation or active control while interacting with a moving tissue simulation target.

In previous research we recorded forces required for interventional cardiac procedures up to 1.5 N (Wagner et al., 2006). We therefore selected 1 N as the target force level, with the 1.5 N level as the upper bound. Based on the literature, this target force is likely greater than the optimal contact force for cardiac ablation (Shah et al., 2010). The 1.5 N force threshold was also selected during preliminary experiments to indicate that the force tracking had diverged and to prevent any damage to the force sensor or catheter mechanisms.

Other possible metrics for determining this error state in addition to a force threshold include a catheter velocity threshold to anticipate instability or limit cycles and a system power function that includes both catheter tip velocity and force. In addition, electrocardiogram (ECG) monitoring can be used to detect ectopic heart beats or arrhythmias in anticipation of abnormal myocardial muscle contractions and withdraw the catheter to a safe position (Berne and Levy, 1997).

4.2. Evaluation results

The catheter system was evaluated using the 3DUS tracking system in a water tank interacting with both the sinusoidal and mitral valve annulus motion target. The use of the
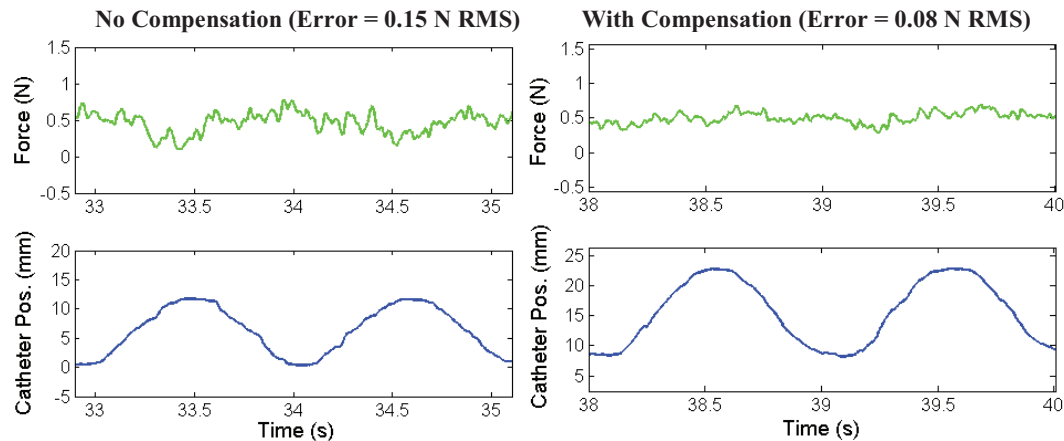
No Compensation (Error = 0.15 N RMS)   **With Compensation (Error = 0.08 N RMS)**

Fig. 13. The force tracking results in a water tank under 3DUS guidance for the sinusoidal target trajectory. Left: Without deadzone or friction compensation (RMS error = 0.15 N). Right: With compensation terms (RMS error = 0.08 N).
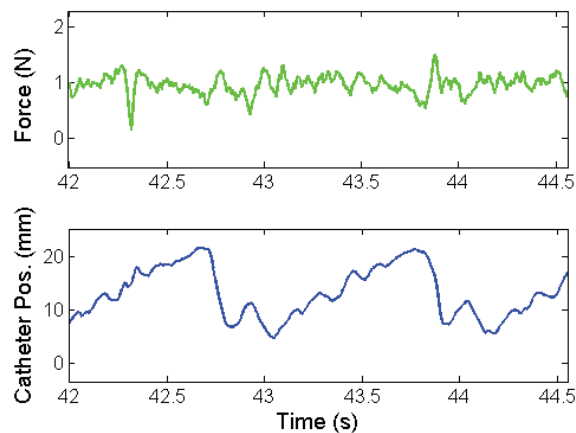

Fig. 14. The force tracking results in a water tank under 3DUS guidance with a mitral valve annulus trajectory target with the compensation terms. Force tracking error = 0.17 N RMS.

Fig. 15. The position-modulation term of the force controller improves the tip trajectory tracking. The three lines are the actual target position, the desired catheter position determined by the force control system, and the EKF-predicted target position from the 3DUS-guidance system.

3DUS complicates the force tracking process because of the importance of the target position prediction, as discussed above in Section 2.1. Even in the controlled environment of the water tank experiment, the system performance varied between each trial due to the quality of the EKF tissue position prediction component of the visual servoing system described in Section 2.1 (Yuen et al., 2010). In spite of these limitations, performance values of 0.08 N RMS errors were achieved for the sinusoidal trajectory (Figure 13). Without friction and deadzone compensation, force tracking results of only 0.15 N RMS were achieved relative to the sinusoidal target (Figure 13). Force control performance values of 0.17 N RMS errors were achieved while interacting with a mitral valve annulus motion simulator with friction and deadzone compensation (Figure 14). The target trajectory for this experiment was generated from human mitral valve annulus data (Kettler et al., 2007). See Figures 13 and 14 for plots of the system performance in these experiments.
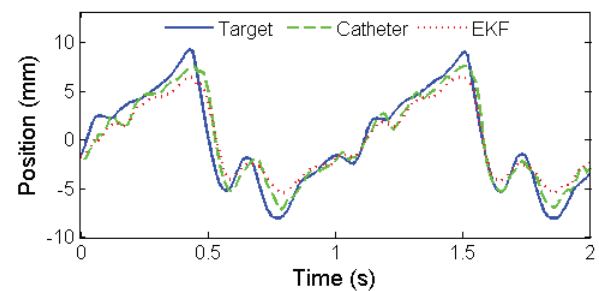
4.3. Motion tracking improvements due to force feedback

In addition to providing force tracking, the catheter control system also improves the position tracking accuracy of the catheter tip. The position trajectory commanded by the 3DUS tracking algorithm follows the true position of the human mitral valve motion simulator with 1.60 mm RMS error. However with the addition of the force feedback controller, the catheter position is accurate to 1.31 mm, an improvement of almost 20%. Figure 15 illustrates this improvement. The catheter trajectory tracks the minima and maxima of the target motion better with the addition of the force feedback modulation controller.

There are two possible explanations for this improved result. First, the backlash compensation method commands the catheter to overshoot the target position at the extremes of the motion trajectory. This behavior would provide improved motion tracking if the 3DUS guidance method was not able to track the extremes of the target motion. The more likely explanation is that the force feedback pushed and pulled the catheter into the correct positions. As the

catheter tip maintains contact with the target, any deviations of the position tracking will result in an increase or decrease of the forces experienced at the catheter tip. The force feedback loop responds to this force change by modulating the catheter tip position and adjusting the catheter trajectory to better match the target. Thus, the force feedback modulation corrects some of the errors of the 3DUS tracking by correcting its position to maintain the constant force on the moving target.

5. Ablation experiments

The final set of experiments presented here evaluates the robotic catheter system's ability to perform a simulated interventional task, maintaining ablation electrode contact against a moving surface while applying a constant force. A number of studies have demonstrated that cardiac ablation efficacy is directly related to the forces applied by the catheter tip and the quality of the electrode–tissue contact (Kalman et al., 1997; Okumura et al., 2007; Shah et al., 2010, 2011). Manually operated catheters do not adequately ablate tissue if they are bouncing or sliding on the tissue surface, in poor contact due to low forces, or creating tissue perforations due to large contact forces (Shah et al., 2010, 2011). The objective of this evaluation was to demonstrate that the robotic catheter system can maintain good target tissue contact and accurately control the applied force in a simulated ablation task. Other representative evaluation tasks that could have also been selected to examine the catheter system include placement of cardiac implants and manipulation of cardiac valve structures (Yuen et al., 2008a; Kesner and Howe, 2011d).

5.1. Evaluation method

The system was evaluated by commanding the catheter to maintain a constant contact force against a moving target. The target was composed of a conductive pad used as the current return path electrode in clinical ablation and electrocautery procedures (REM Polyhesive II Patient Return Electrode, Tyco Healthcare, Gosport, UK) backed with compliant foam (thickness: 25 mm, approximate stiffness: 0.1 N/mm). The target was translated along a 12 mm amplitude at a frequency of approximately 1 Hz (60 beats per minute). Two motion patterns were tested: a sinusoidal trajectory and a human mitral annulus trajectory (Kettler et al., 2007). The ablation quality was approximated by measuring the electrical resistance between the catheter tip electrode and the return electrode pad using an instrumented voltage divider designed to match the approximate resistance range of the catheter tip–target interaction (Figure 16). For the purposes of these validation experiments, resistance also provides an independent measure of contact quality that does not rely on ultrasound imaging. No ablation energy was applied during the electrical resistance measurements.
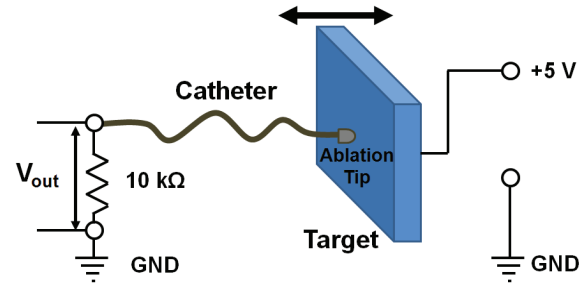

Fig. 16. The catheter ablation experimental setup. The moving target was connected to a 5 V DC signal and the catheters were instrumented with a voltage divider to measure the contact resistance. Resistance measurements were used to evaluate tip contact quality for both a manual catheter and the robotic catheter system.

The water tank environment was used to allow the 3DUS guidance system to visualize the catheter and target.

The evaluation experiment was conducted using both the robotic catheter and a commercial manual ablation catheter (RF Marinr MCXL, Medtronic, Minneapolis, MN) for comparison. A manual catheter was select as a passive mechanical equivalent to act as a baseline for comparison in order to analyze the performance of the robotic catheter. For the manual catheter, a load cell was also added to the target to record the forces applied by the catheter tip (LCFD-1KG, Omega Engineering, Stamford, CT; range: 10 N, accuracy: ±0.015 N). The robotic catheter was instrumented with the force-sensing ablation end effector and was operated under force control with 3DUS guidance. Both catheters were rigidly braced 100 mm from the ablation tip at orientations perpendicular to the plane of the moving target. The manual catheter was positioned so its ablation electrode was able to remain in contact during the entire target trajectory (Figure 17). It should be noted that this experimental setup does not accurately simulate all aspects of intracardiac ablation, including the compliance of the vessels in the heart, the instrument orientation relative to the moving tissue structures, and the electrical impedances of the cardiac environments and human body.

To measure the resistance, 5 V DC was applied to the patient return electrode and a voltage divider was created at the proximal end of the catheters to measure the ablation resistance (Figure 16). As the contact between the catheter and the target changed due to variations of the contact force or tip position, the resistance between the catheter electrode and the return electrode pad also changed. This resistance, R_{abl}, can be calculated from the resulting output of the voltage divider, V_{out}:

$$R_{abl} = \frac{5V}{V_{out}} \times 10 \text{ k}\Omega - 10 \text{ k}\Omega = \left(\frac{5V}{V_{out}} - 1 \right) \times 10 \text{ k}\Omega$$
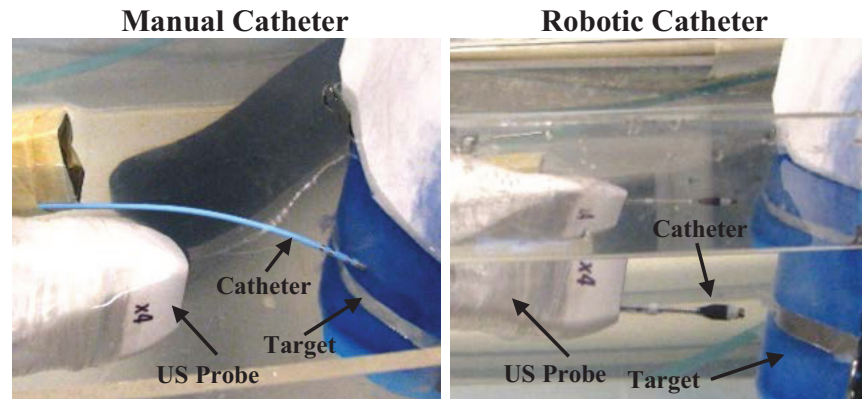
(4)

Manual Catheter   Robotic Catheter

Fig. 17. The water tank setup for the manual catheter (top) and the robotic catheter (bottom). Both images show the catheters, the white 3DUS imaging probe, and the motion target.
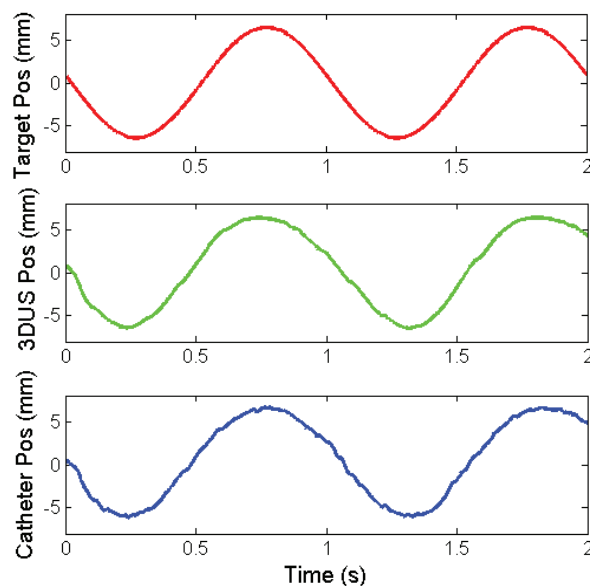

Fig. 18. The position trajectories during the robotic catheter experiment: (top) the real target trajectory; (middle) the trajectory determined by the 3DUS tracking system; (bottom) the force-modified position commanded by the control system.

5.2. Results

Figure 18 presents the position trajectories of the 3DUS tracking system, robotic catheter, and motion simulator during the experiments. Figure 19 presents typical results of the ablation experiment on the sinusoidal motion target. Both the manual and robotic catheters were in contact with the moving target for over 5 s during each trial.

The manual catheter was not able to apply a constant force or maintain a constant resistance. The reason for the manual catheter's poor performance was because the motion of the target caused the manual catheter ablation tip to slide and tilt relative to the target surface as the motion simulator pushed on the catheter and caused it to buckle. Compliance is a desirable feature in manual

catheters because it prevents them from applying large forces and perforating cardiac tissue. In addition, compliance also allows the catheter to remain in contact despite large motion of cardiac structures. However, this bending compliance makes it challenging to achieve reliable ablation performance. As shown in Figure 19, the manual catheter generated peak-to-peak resistance variations of over 20 kΩ and peak-to-peak force variations of over 0.45 N, approximately 125% of the mean force value (0.37 N).

The robotic catheter, in contrast to the manual catheter, achieved almost constant resistance values while maintaining a desired force of 1 N with a force tracking error of 0.11 N RMS. The RMS variation of the resistance value for the robotic catheter was 0.25 kΩ, 97% less than the RMS variation of 9.88 kΩ for the manual catheter system. The robotic catheter was able to achieve this level of performance because the 3DUS-guided motion compensation system and the force control algorithm enabled the ablation tip to maintain consistent contact with the target despite the fast motion (Figure 19).

6. Discussion

These results demonstrate that image-guided motion compensation and force control can enable a catheter to maintain a constant, safe force against a moving target, a potentially key feature for improving ablation quality. The system was able to apply a constant force while maintaining a near-constant contact resistance with the ablation end effector on a moving target. In contrast, the force and electrical contact provided by the passive manual catheter in the same experimental setup varied greatly. This variation can primarily be attributed to the buckling, sliding, and tilting behavior of the manual catheter tip due to the target motion. The 3DUS motion tracking enabled the robotic catheter to compensate for the target motion and maintain good ablation electrode contact without the buckling behavior of the manual catheter. It should be noted that a skill clinician operated the manual catheter would have achieved better results
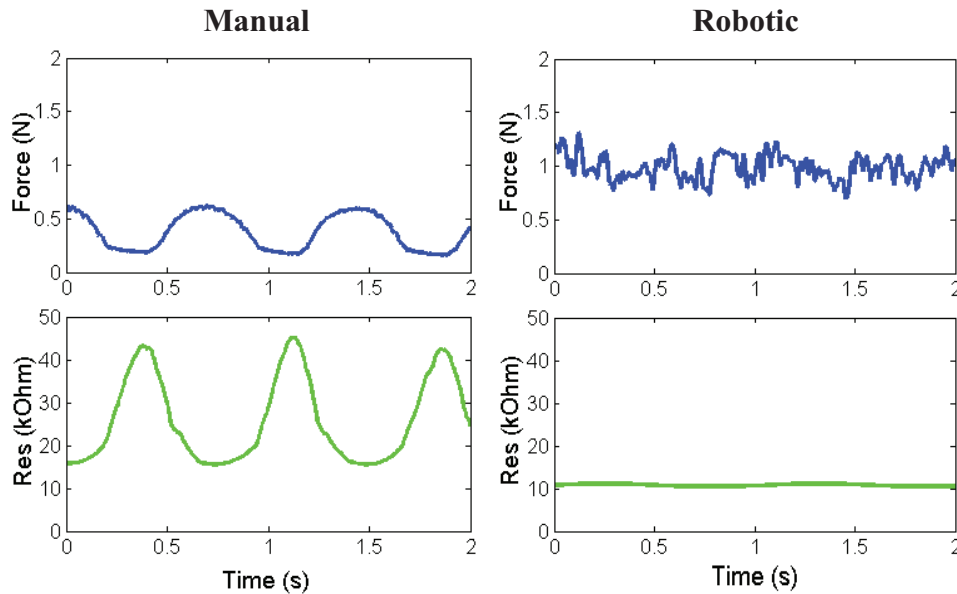
Manual

Robotic

Fig. 19. A comparison of the contact resistance and interaction forces between a conductive target and a manual catheter (left) and the robotic catheter system (right). The manual catheter applies a force and resistance that vary with the motion of the target. In contrast, the robotic catheter achieved consistent resistance with the moving target while applying a constant force.

than the passive mechanical equivalent through improved catheter tip position manipulation and actively adjusting the angle of the catheter relative to the moving target surface. The required position and force accuracy for the robotic catheter system depends on the specific clinical application, the required quality of interventional procedure, and the force levels that will result in tissue damage for the application. An argument can be made that an accuracy roughly similar to a skilled surgeon operating on a stopped heart with an actuated instrument would be appropriate for this work. Thus, a position accuracy of approximately 1 mm was deemed sufficient (Falk, 2002). Force accuracy is a more challenging value to select. A force accuracy equivalent or better than a human hand performing a dexterous manipulation task is appropriate. Jones and Piateski (2006) found that for finger and hand grasping tasks, an average force accuracy of roughly 0.5 N was attainable for a 2–10 range. Our system will apply smaller forces than this range, thus an accuracy of under 0.25 N is sufficient.

One insight from this work is that multiple forms of sensor information are required to command a catheter to safely and effectively interact with the moving target. Force sensing alone is not sufficient for the catheter to track the target motion, as described by Kesner and Howe (2011c). This is due to the fact that the catheter performance limitations of backlash and friction prevent the system from responding fast enough to the quick tissue motion using only force feedback. Motion tracking must also be used to overcome these limitations and maintain system stability (Kesner and Howe, 2011c). The image guidance provides an approximation of the desired position trajectory for the tip of the catheter and the force feedback introduces minor

adjustments to the tip position to regulate and maintain the tool-tissue interactions forces. This insight is demonstrated with the 20% position tracking improvements provided by the combination of the force control system and 3DUS motion tracking while following the mitral valve annulus motion simulator, as shown in Figure 15. Without either 3DUS guidance or force sensing, the catheter would be unable to maintain the consistent ablation electrode contact and could either penetrate or retract from the target surface.

In addition to 3DUS, other position tracking systems are available for intracardiac interventions. For example, ablation impedance tracking systems, such as the CARTO system (Biosense Webster, Inc., Diamond Bar, CA), use a combination of the ablation catheter position from electromagnetic tracking and the electrical impedance values to perform cardiac mapping and ablation procedures. While these systems do assist clinicians to guide ablation procedures, they do not track the physical position of the moving cardiac tissue in real time to allow a catheter to compensate for the motion or apply a constant force against moving cardiac structures. 3DUS enables the advantages of imaging and tracking both the catheter and soft tissue to allow for safe manipulation of fast-moving cardiac tissues.

Although the experimental results demonstrate that the robotic catheter system is able to apply a constant force while maintaining a consistent ablation contact, there are a number of limitations in this initial validation study due to the challenges of accurately simulating *in vivo* cardiac ablation in a laboratory setting. First, measuring the DC resistance of the contact does not consider the electrical frequency response of the cardiac tissue at the 500 kHz frequency used by the RF energy generator. In addition,

the system was tested in water instead of electrically-conductive blood or saline, which alters the electrode conduction properties. Finally, the experimental setup did not approximate the exact mechanics of intracardiac ablation, including the compliance of the vessels in the heart and the tool orientation relative to the moving tissue structures. The manual catheter performance depends on its orientation with respect to the moving tissue target, although similar fluctuations in force and resistance would have resulted for other orientations. We anticipate that these issues will not impair the demonstrated advantages of the robotic system because of the known properties of the ablation process and the success of previous *in vivo* tests of the image guidance systems (Yuen et al., 2008a; Kesner et al. 2010; Kesner and Howe, 2011d).

7. Conclusions

This paper presents the experimental evaluation of a robotic catheter system for interacting with the beating heart. The specific medical application selected for this system is performing tissue ablation on a moving cardiac structure. The system uses motion compensation and force feedback to maintain a constant force and contact resistance on a moving target. The experimental results presented here demonstrated that the robotic system is able to apply a constant force on a moving target with 0.08 N RMS error. In addition to accurately controlling the catheter-tissue interaction forces, the system is able to maintain consistent ablation electrode contact against a translating motion simulator with a 97% reduction in RMS resistance variation over a passive and rigidly fixed manual catheter. This ablation result can be explained by the fact that a compliant manual catheter slides and buckles while in contact with a quickly moving structure, such as the actively contracting heart wall, while the robotic catheter actively compensates for the motion and regulates the interaction forces. Finally, the combination of force feedback and 3DUS guidance improves the trajectory tracking accuracy by adjusting the catheter motion due to the forces experienced at the catheter tip while interacting with the moving target.

Future work in this project will focus on the demonstration and evaluation of the technology in an *in vivo* setting. While the motion compensation and robotic catheter system has been demonstrated previously *in vivo* (Yuen et al., 2008a; Kesner et al., 2010; Kesner and Howe, 2011d), the force control ablation system has not yet been tested inside a beating heart. One possible challenge the system will encounter *in vivo* is how to respond as the tissue stiffness changes over the course of the heart cycle. In addition, safety issues such as system stability and preventing tissue collisions will need to be further investigated. The project objective is to enable a range of beating heart surgical procedures with a catheter, and the ablation application explored here is a first step toward this ultimate goal.

References

Baim DS (2005) *Grossman's Cardiac Catheterization, Angiography, and Intervention*. Philadelphia, PA: Lippincott Williams & Wilkins.

Bebek O and Cavusoglu M (2007) Intelligent control algorithms for robotic assisted beating heart surgery. *IEEE Transactions on Robotics* 23(3): 468–480.

Berne RB and Levy MN (1997) *Cardiovascular Physiology*. 7th ed. Mosby-Year.

Beyar R (2010) Navigation within the heart and vessels in clinical practice. *Annals of the New York Academy of Sciences* 1188(1): 207–213.

Camarillo DB, Milne CF, Carlson CR, et al. (2008) Mechanics modeling of tendon-driven continuum manipulators. *IEEE Transactions on Robotics* 24(6): 1262–1273.

Chiaverini S, Siciliano B and Villani L (1999) A survey of robot interaction control schemes with experimental comparison. *IEEE/ASME Transactions on Mechatronics* 4(3): 273–285.

Eppinger S and Seering W (1987) Understanding bandwidth limitations in robot force control. In: *IEEE International conference on robotics and automation*, pp. 904–909. IEEE.

Falk V (2002) Manual control and tracking – a human factor analysis relevant for beating heart surgery. *The Annals of Thoracic Surgery* 74(2): 624–628.

Ginhoux R, Gangloff J, de Mathelin M, et al. (2005) Active filtering of physiological motion in robotized surgery using predictive control. *IEEE Transactions on Robotics* 21(1): 67–79.

Huang SK, Huang SKS and Wilber DJ (2000) *Radiofrequency Catheter Ablation of Cardiac Arrhythmias: Basic Concepts and Clinical Applications*. Wiley-Blackwell.

Jayender J, Azizian M and Patel RV (2008) Autonomous image-guided robot-assisted active catheter insertion. *IEEE Transactions on Robotics* 24(4): 858–871.

Jones LA and Piateski E. 2006. Contribution of tactile feedback from the hand to the perception of force. *Experimental Brain Research* 168(1): 298–302.

Kalman JM, Fitzpatrick AP, Olgin JE, et al. (1997) Biophysical characteristics of radiofrequency lesion formation in vivo: dynamics of catheter tip–tissue contact evaluated by intracardiac echocardiography. *American Heart Journal* 133(1): 8–18.

Kesner SB and Howe RD (2010) Design and control of motion compensation cardiac catheters. In: *IEEE International conference on robotics and automation*, pp. 1059–1065. IEEE.

Kesner SB and Howe RD (2011a) Design principles for rapid prototyping forces sensors using 3-D printing. *IEEE/ASME Transactions on Mechatronics* (99): 1–5.

Kesner SB and Howe RD (2011b) Discriminating tissue stiffness with a haptic catheter: feeling the inside of the beating heart. In: *World haptics conference*, Istanbul, Turkey, 21–24 June 2011, pp. 13–18. IEEE.

Kesner SB and Howe RD (2011c) Force control of flexible catheter robots for beating heart surgery. In: *IEEE International conference on robotics and automation (ICRA)*, pp. 1589–1594. IEEE.

Kesner SB and Howe RD (2011d) Position control of motion compensation cardiac catheters. *IEEE Transactions on Robotics* (99): 1–11.

Kesner SB and Howe RD (2012) Motion compensated catheter ablation of the beating heart using image guidance and force control. Quebec City, Canada.

Kesner SB, Yuen S and Howe R (2010) Ultrasound Servoing of Catheters for Beating Heart Valve Repair. *Information Processing in Computer-Assisted Interventions* 6135: 168–178.

Kettler DT, Plowes RD, Novotny PM, et al. (2007) An active motion compensation instrument for beating heart mitral valve surgery. In: *IEEE/RSJ International conference on intelligent robots and systems*, pp. 1290–1295. IEEE.

Maples J and Becker J (1986) Experiments in force control of robotic manipulators. In: *IEEE International conference on robotics and automation*, pp. 695–702. IEEE.

Murkin JM, Boyd WD, Ganapathy S, et al. (1999) Beating heart surgery: why expect less central nervous system morbidity? *The Annals of Thoracic Surgery* 68(4): 1498–1501.

Nakamura Y, Kishi K and Kawakami H (2001) Heartbeat synchronization for robotic cardiac surgery. In: *IEEE International conference on robotics and automation*, pp. 2014–2019. IEEE.

Novotny PM, Stoll JA, Dupont PE, et al. (2007a) Real-time visual servoing of a robot using three-dimensional ultrasound. In: *IEEE International conference on robotics and automation*, pp. 2655–2660. IEEE.

Novotny PM, Stoll JA, Vasilyev NV, et al. (2007b) GPU based real-time instrument tracking with three-dimensional ultrasound. *Medical Image Analysis* 11(5): 458–464.

Objet Geometries Ltd (2010) *FullCure870 VeroBlack Data Sheet*. Objet Geometries Ltd.

Okumura Y, Johnson S and Packer D (2007) An analysis of catheter tip/tissue contact force-induced distortion of three-dimensional electroanatomical mapping created using the sensei robotic catheter system. *Heart Rhythm* 4: S318.

Prisco GM (2012) *Fiber Optic Shape Sensing*. Patent US 8116601 B2. Available at: www.google.com/patents/US8116601

Richa R, Bó APL and Poignet P (2010) Beating heart motion prediction for robust visual tracking. In: *IEEE International conference on robotics and automation*, pp. 4579–4584. IEEE.

Roach GW, Kanchuger M, Mangano CM, et al. (1996) Adverse cerebral outcomes after coronary bypass surgery. *New England Journal of Medicine* 335(25): 1857–1864.

Shah DC, Lambert H, Langenkamp A, et al. (2011) Catheter tip force required for mechanical perforation of porcine cardiac chambers. *Europace* 13(2): 277.

Shah DC, Lambert H, Nakagawa H, et al. (2010) Area under the real-time contact force curve (force–time integral) predicts radiofrequency lesion size in an *in vitro* contractile model. *Journal of Cardiovascular Electrophysiology* 21(9): 1038–1043.

Townsend W and Salisbury J Jr (1987) The effect of coulomb friction and stiction on force control. In: *IEEE International Conference on robotics and automation*, pp. 883–889. IEEE.

Wagner CR, Perrin DP, Howe RD, et al. (2006) Force feedback in a three-dimensional ultrasound-guided surgical task. In: *14th symposium on haptic interfaces for virtual environment and teleoperator systems*, 25–26 March 2006, pp. 43–48. IEEE.

Webster JG (1988) *Tactile Sensors for Robotics and and Medicine*. New York: John Wiley & Sons, Inc.

Wilson E, Yaniv Z, Lindisch D, et al. (2008) A Buyer's Guide to Electromagnetic Tracking Systems for Clinical Applications. In: *Proceedings of the SPIE, Volume 6819*. Cardiff: SPIE.

Yuen SG, Kesner SB, Vasilyev NV, et al. (2008a) 3D ultrasound-guided motion compensation system for beating heart mitral valve repair. In: *Proceedings of medical image computing and computer-assisted intervention (MICCAI)*, New York, NY, 6–10 September 2008.

Yuen SG, Kettler DT, Novotny PM, et al. (2009) Robotic motion compensation for beating heart intracardiac surgery. *The International Journal of Robotics Research* 28(10): 1355.

Yuen SG, Kettler DT, Novotny PM, et al. (2010) Robotic tissue tracking for beating heart mitral valve surgery. *Medical Image Analysis* 17: 1236–1242.

Yuen SG, Novotny PM and Howe RD (2008b) Quasiperiodic predictive filtering for robot-assisted beating heart surgery. In: *IEEE International conference on robotics and automation*, pp. 3875–3880. IEEE.